Global NEST Journal, Vol 9, No 2, pp 117-131, 2007

A WIND-DRIVEN HYDRODYNAMIC AND POLLUTANT TRANSPORT MODEL

IOANNIS K. TSANIS*
USAMA SAIED

Department of Civil Engineering
McMaster University, Hamilton, Ontario, L8S 4L7, Canada

Received: 04/03/05
Accepted: 14/07/05

*to whom all correspondence should be addressed:
e-mail: tsanis@mcmaster.ca

ABSTRACT
A program is developed that includes two hydrodynamic models, a 2D depth-averaged (2DH) and a Quasi-3D (Q3D), and a pollutant transport model that uses a 1st order upwinding and a 3rd order QUICKEST numerical schemes. Several tests were performed in two test basins in order to examine the performance of the above models. The Q3D model is successfully applied to Lake Ontario, using a 4-km-square grid, to simulate the wind-induced circulation. Simulations of pollutant transport show that the 1st order upwinding scheme can be used for estimating pollutant concentrations near the pollutant source in the case of continuous point source. However, numerical diffusion affects the estimates further downstream the pollutant source. Therefore, higher order schemes such as the third order QUICKEST scheme are required for estimating pollutant concentration at these locations.

KEYWORDS: Lake circulation model, pollutant transport model, wind-driven currents, Lake Ontario

INTRODUCTION

Hydrodynamic and pollutant transport modeling in closed water bodies require a detailed knowledge of the transport processes that exist within the body. Essential elements for life and productivity such as oxygen, heat and nutrients are transported and dispersed through these processes. These processes cause the dilution of pollutants though mixing with the ambient water resulting in their reduced impact on nearshore areas.

The geometry of the closed water bodies such as lakes reveal that the horizontal length scale is several order of magnitude greater than the vertical length scale. The induced circulation can be hydraulically or wind-driven. For the case of hydraulically-driven circulation, the current vertical distribution is almost uniform over the depth with sharp gradients existing only at the bottom (Blaisdell *et al*., 1991). The current driven vertical velocity profile can be treated as if the whole water column is a boundary layer and therefore the Prandtl-von Karman logarithmic velocity profile applies. In this case, the two-dimensional horizontal depth-averaged model can successfully simulate the depth-averaged current distribution. In the case of wind-driven flows the vertical current distribution is countercurrent with the current in lower layers moving in opposite direction to wind. In order to incorporate the effects of the non-uniform velocity in the vertical plane, Koutitas (1988) developed the so-called quasi-three-dimensional (Q3D) wind driven circulation model (Wu, 1993). This model, basically, solves the depth-averaged Navier-Stokes equations assuming a parabolic velocity profile in the vertical, to be consistent with the wind driven velocity profiles. The quasi-three-dimensional model has the advantage of simplicity, requires short computational time and implicitly implements the vertical current distribution.

Following the introduction, the analytical background of circulation and pollutant transport models are presented. The functionality of the model and the corresponding program description with applications to two basins under different meteorological and environmental condi-

tions is also presented followed by the application of Q3D model and the pollutant transport models to Lake Ontario with the appropriate conclusions.

ANALYTICAL BACKGROUND

Circulation Models

Two-dimensional horizontal depth-averaged circulation model (2DH)

Given the large horizontal dimensions (km) relative to the vertical (m) in closed water bodies, the vertical velocities and accelerations are small relative to the horizontal components (Csanady, 1982). Therefore the vertical equation of motion may be replaced by the hydrostatic pressure approximation. The resulting depth-averaged Navier-Stokes equations become (Koutitas, 1988):

$$\frac{\partial U}{\partial t} + U\frac{\partial U}{\partial x} + V\frac{\partial U}{\partial y} = -g\frac{\partial \zeta}{\partial x} + fV + \frac{\tau_{sx}}{\rho h} - \frac{\tau_{bx}}{\rho h} \quad (1)$$

$$\frac{\partial V}{\partial t} + U\frac{\partial V}{\partial x} + V\frac{\partial V}{\partial y} = -g\frac{\partial \zeta}{\partial y} - fU + \frac{\tau_{sy}}{\rho h} - \frac{\tau_{by}}{\rho h} \quad (2)$$

$$\frac{\partial \zeta}{\partial t} + \frac{\partial}{\partial x}(UH) + \frac{\partial}{\partial y}(VH) = 0 \quad (3)$$

where ζ is the water surface elevation above the mean water level; h is the water depth; H is the total depth of water (i.e. $H=h+\zeta$); U, V are the depth-averaged velocity components in x and y directions respectively; f is the Coriolis parameter; ρ is the water density; τ_{sx} and τ_{sy} are the shear stresses at the water surface in the x and y directions respectively, which represent the vertical boundary condition as follows:

$$\tau_{sx} = \rho C_s W_x \sqrt{W_x^2 + W_y^2} \quad (4)$$

$$\tau_{sy} = \rho C_s W_y \sqrt{W_x^2 + W_y^2} \quad (5)$$

where C_s is the surface friction coefficient (typically of the order of 10^{-6} assumed 0.0000018); W_x and W_y are the wind speeds in x and y directions [m s^{-1}], respectively. Similarly, the bed friction terms (τ_{bx}, τ_{by}) are expressed by quadratic forms as follows:

$$\tau_{bx} = \rho C_b U \sqrt{U^2 + V^2} \quad (6)$$

$$\tau_{by} = \rho C_b V \sqrt{U^2 + V^2} \quad (7)$$

where C_b is the bottom friction coefficient (chosen to be 0.0025).

In the previous model, the depth averaged approximation of the convective terms should have contain additional terms for horizontal momentum dispersion for the case of nonlinear vertical velocity profiles, which is the case for wind driven flows (Koutitas, 1988). In addition, Equations (6) and (7) imply that when the depth mean velocity components are zero, the friction terms are suppressed. However, for wind generated currents, even in the case of zero depth-mean velocities, the near bed shear is not negligible.

Quasi-three dimensional circulation model (Q3D)

The advantage of this model is that it can provide the current distribution at any depth as well as the depth-averaged current structure. The equations of motion in the x and y directions and the mass continuity are simplified under the assumption that a) the water is incompressible and homogeneous, and b) the flow is quasi-hydrostatic. The second assumption is based on the fact that the horizontal dimension of the flow domain is several order of magnitude larger than the vertical dimension (depth). The assumption of nearly horizontal flow is realistic and simplifies the model by excluding the vertical velocity component “w” from the main unknown functions and leads to a hydrostatic pressure distribution. In order to incorporate the effects of the non-uniform velocities in the vertical, especially in the wind-induced cases, a

parabolic velocity profile in the vertical is assumed and the coefficients are determined from the boundary conditions at the surface, and the bottom. The velocity profile is defined as follows:

$$u(z) = \left(\frac{3\tau_{sx}h}{4\rho\nu} - \frac{3U}{2}\right)\left[\left(\frac{z}{h}\right)^2 - 1\right] + \frac{\tau_{sx}h}{\rho\nu}\left(\frac{z}{h} + 1\right) \tag{8}$$

$$v(z) = \left(\frac{3\tau_{sy}h}{4\rho\nu} - \frac{3V}{2}\right)\left[\left(\frac{z}{h}\right)^2 - 1\right] + \frac{\tau_{sy}h}{\rho\nu}\left(\frac{z}{h} + 1\right) \tag{9}$$

where the z-axis has its origin coincides with the water surface; ν is the eddy viscosity at the surface. A constant eddy viscosity is assumed in order to be consistent with the parabolic velocity profile (Koutitas, 1988).

Based on the velocity component distributions given by Equations (8) and (9), the convective terms are evaluated. The two-dimensional model, improved with respect to the horizontal momentum dispersion and the bed friction for wind generated circulation, becomes (Koutitas, 1988),

$$\frac{\partial U}{\partial t} + (1.2U + \frac{\tau_{sx}h}{40\rho\nu})\frac{\partial U}{\partial x} + (1.2V + \frac{\tau_{sy}h}{40\rho\nu})\frac{\partial U}{\partial y} = -g\frac{\partial \zeta}{\partial x} + fV + \frac{\tau_{sx}}{\rho h} - (3\bar{\lambda}\frac{U}{h}\sqrt{\frac{\tau_{sx}}{\rho}} - 0.5\frac{\tau_{sx}}{\rho h}) \tag{10}$$

$$\frac{\partial V}{\partial t} + (1.2U + \frac{\tau_{sx}h}{40\rho\nu})\frac{\partial V}{\partial x} + (1.2V + \frac{\tau_{sy}h}{40\rho\nu})\frac{\partial V}{\partial y} = -g\frac{\partial \zeta}{\partial y} - fU + \frac{\tau_{sy}}{\rho h} - (3\bar{\lambda}\frac{V}{h}\sqrt{\frac{\tau_{sy}}{\rho}} - 0.5\frac{\tau_{sy}}{\rho h}) \tag{11}$$

$$\frac{\partial \zeta}{\partial t} + \frac{\partial}{\partial x}(UH) + \frac{\partial}{\partial y}(VH) = 0 \tag{12}$$

where τ_{sx} and τ_{sy} are the shear stresses at the water surface in the x and y directions respectively and are given by equations (4) and (5).

The "$\bar{\lambda}$" is a coefficient used to determine the eddy viscosity "ν" through this equation;

$$\nu = \bar{\lambda} h\sqrt{\frac{\tau_s}{\rho}} \quad ; \tau_s = \sqrt{\tau_{sx}^2 + \tau_{sy}^2} \; ; O\left[\bar{\lambda}\right] = 0.1 \tag{13}$$

Equations (8) and (9) permit the computation of the current pattern at any depth, i.e., the free surface velocity components (z=0) are given by:

$$u_{surf} = \frac{3U}{2} + \frac{\tau_{sx}h}{4\rho\nu} \tag{14}$$

$$v_{surf} = \frac{3V}{2} + \frac{\tau_{sy}h}{4\rho\nu} \tag{15}$$

The above model was successfully verified and applied to Lake St. Clair (Wu and Tsanis, 1991) and the model was applied to all the Canadian Great Lakes (Tsanis and Wu, 1991). The quasi-three-dimensional (Q3D) model can estimate the depth averaged velocities as well as the current structure in the vertical direction.

Numerical integration

A centered finite difference scheme is used to numerically describe the spatial derivatives. The flow domain is discretized on a space-staggered grid, and the solution of the finite difference system is achieved using an explicit leap-frog algorithm for the time integration. The Courant-Friedrichs-Lewy (CFL) criteria controls the applied time step as follows (Blaisdell *et al.*, 1991):

$$\Delta t < \frac{\Delta x}{\sqrt{2gh_{max}}} \tag{16}$$

where h_{max} is the maximum depth in the calculation domain.

As calculation progresses, the kinetic energy per unit density contained in the basin is calculated at each time step by summing the square of the grid-point velocities U and V:

$$E^n = \frac{1}{8}\sum_{i=1}^{imax}\sum_{j=1}^{jmax}[(U_{i,j}^n + U_{i+1,j}^n)^2 + (V_{i,j}^n + V_{i,j+1}^n)^2]h_{i,j}\Delta x^2 \tag{17}$$

where i, j and n indices refer to the x, y and time dimensions, respectively. Steady state is achieved when the ratio between the difference in kinetic energy between time steps falls between a certain accuracy (typically 1×10^{-7}).

Because the shortest wavelength component which can be described by the computational mesh is $2\Delta x$, and because of the nonlinearity of the velocity field, aliasing occurs (Roache, 1972). Therefore, in order to simulate the transfer of turbulent kinetic energy to scales smaller than $2\Delta x$, and to control grid dispersion induced by the leap-frog scheme, an artificial dissipative mechanism is introduced (Blaisdell *et al.*, 1991). Because it is the long wavelength phenomenon that is of interest herein (surface elevations and velocities) and not the subscale phenomenon, in combination with the fact that some damping of the turbulent motions occurs naturally, some degree of horizontal smoothing is acceptable and, in fact, desirable. The damping is incorporated into the solution of the temporal derivatives in the following manner:

$$\frac{\partial U}{\partial t} = \frac{U_{ij}^{n+1} - U_{ij}^n}{\Delta t} - \frac{(1-t_h)\Delta x^2}{4\Delta t}\frac{\partial^2 U}{\partial x^2} - \frac{(1-t_h)\Delta y^2}{4\Delta t}\frac{\partial^2 U}{\partial y^2} \tag{18}$$

where t_h is the smoothing factor, which may be related to the horizontal eddy viscosity by the following relation:

$$\upsilon_h = \frac{(1-t_h)\Delta x^2}{4\Delta t} \tag{19}$$

Pollutant Transport Model

The two-dimensional depth-averaged pollutant transport equation for a non-conservative pollutant is:

$$\frac{\partial C}{\partial t} + \frac{\partial (CU)}{\partial x} + \frac{\partial (CV)}{\partial y} = \frac{\partial}{\partial x}(D_x \frac{\partial C}{\partial x}) + \frac{\partial}{\partial y}(D_y \frac{\partial C}{\partial y}) - \lambda C \tag{20}$$

where D_x, D_y are the dispersion coefficients; U, V are the depth mean velocities in the x and y directions, respectively; λ is the decay coefficient (s^{-1}). The boundary conditions completing the model are; (a) solid boundaries - zero normal flux, (b) free transmission boundaries - uniform flux, and (c) pollution sources - pollutant concentration is known. A first order decay coefficient "λ" is used to model the decay and production of a non-conservative pollutant due to the following: (1) biological growth or decay of bacteria, (2) chemical reaction with environment (oxidation, etc.), and (3) settlement of flocculated pollutant molecules. Two methods are used for the approximation of the concentration at the faces of the grid cells. The 1st is the first-order upwinding scheme, which usually suffers from numerical diffusion due to the inclination of the velocity vectors with respect to the grid lines. The second is the third order QUICKEST scheme, which reduces the numerical diffusion.

PROGRAM DESCRIPTION

The main program consists of two models; circulation model and pollutant transport model. The circulation model has two options (a) employs the quasi-three-dimensional model and (b) employs the conventional horizontal depth-averaged model. The pollutant transport model is a depth-averaged model and has two options as well (a) employs the 1st order upwinding-differencing scheme and (b) employs the QUICKEST scheme. The user can choose different time steps and different simulation times with the above options.

Different parameters have to be set by the user to control the following: (1) choose to run both models simultaneously or separately, (2) choose weather the program stops the circulation

model after reaching the steady state or continues till the end of the simulation time, (3) choose the type of the pollutant (instantaneous / continuous), (4) choose the time of introducing the pollutant. The model allows the user to input variable wind conditions as well as steady wind. A two hours warming up period is set for the wind and for the discharge in/out the lake. Table 1 shows the main parameters of the program.

Table 1. Model Parameters

dt1	Time step for the circulation model (second)
dt2	Time step for the pollutant transport model (second)
tlast	Simulation time for the circulation model (hours)
tlast2	Simulation time for the pollutant transport model (hours)
nnd	Number of source pollutants.
cnd(k)	Concentration of point sources.
modtype	=1 if circulation and pollutant transport models are running simultaneously. =2 if they are running separately.
modsteady	=1 The circulation model will stop after reaching the steady state =2 The circulation model will stop at the end of the simulation time.
ncmodel	=1 The pollutant transport model employs the First order upwinding method =2 The pollutant transport model employs the QUICKEST method
pointtype	=1 Continuous point source =2 Instantaneous point source
tpoint	Time of introducing the instantaneous point source (hours)
n_model	=1 For 2D depth averaged circulation model =2 For Quasi-three-dimensional model
ncmodel	=1 First order upwinding scheme =2 QUICKEST scheme

The program is designed to write its output as ASCI files, which can be read by Tecplot. The output files can be classified as two-dimensional output or one-dimensional output. The first includes the spatial dependent variables such as velocity, concentration, and water surface elevation. The later includes the vertical velocity profile, the time concentration curves, the kinetic energy versus time curve and the cross-section data (i.e. velocity, concentration, etc.). A set of Tecplot macros were developed in order to prepare the required figures. These macros run in batch mode so that the program with the macros produces a fully objective-oriented package.

TEST CASE

In order to test the behavior of the circulation model and to compare between the different hydrodynamic and pollutant transport models, two test basins have been assumed. Figure (1) shows the two basins and the horizontal grid. Table (2) summarizes the test-case runs.

Table 2. Test-case runs

Run#	Basin	Model Used		Time Step		Simulation Time		Release Time (hr)	Force
		Hydr.	Pol.	dt1 (s.)	dt2 (s.)	Hydr.	Pol.		
1	A	Q3D	---	0.5	---	5	---	---	-1
2	A	2DH	---	0.5	---	5	---	---	
3	B	Q3D	---	0.5	---	5	---	---	
4	B	2DH	---	0.5	---	5	---	---	
5	A	Q3D	---	0.5	---	5	---	---	50 $m^3 s^{-1}$ Discharge at (2,5)
6	A	2DH	---	0.5	---	5	---	---	
7	A	Q3D	Up-wind	0.5	0.5	3	10	1 @ (2,5)	
8	A	Q3D	QUIC KEST	0.5	0.5	3	10	1 @ (2,5)	

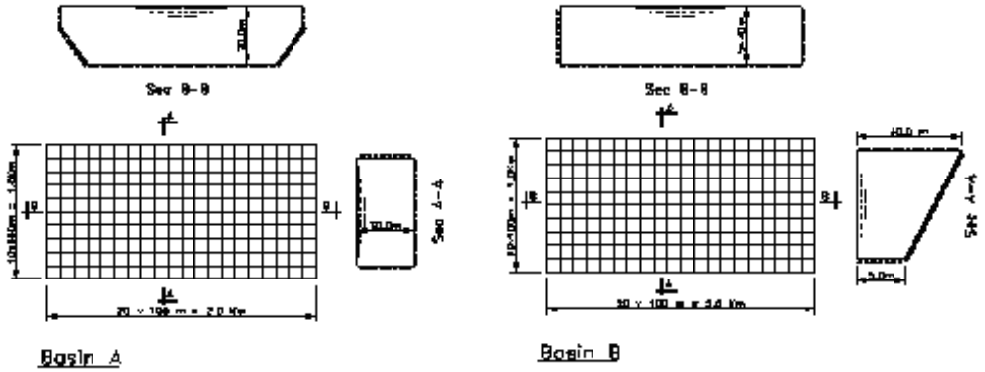

Figure 1. Definition of the test Basins

Figures 2 and 3 show the circulation patterns, the total kinetic energy of flow, and the wind set-up after running the conventional depth averaged model and the Q3D model for basins A and B. There are two resulting circulation cells in basin A due to rectangular cross-section while in basin B there is one clockwise circulation cell due to cross-section with the sloping bottom The Q3D model results in higher free surface gradients balancing both the free surface shear and the bed shear and the total kinetic energy is therefore higher in the case of the Q3D model. Figure 4 shows the vertical velocity profile for two points within the basin A. The Q3D model can resolve the countercurrent nature of the flow.

The Q3D model results in a surface velocity direction in almost the same direction of wind, because the Coriolis force is calculated only for the depth-averaged velocity. However, practically, due to different Coriolis forces for different levels, the Ekman spiral effect results in a surface velocities deflected 45° clockwise from the wind direction in the Northern hemisphere (Ekman, 1905). The fully three dimensional model developed by Shen and Tsanis (1995) accounts for this phenomenon.

The 2DH model is a good approximation for the case of hydraulic currents, where the wind is absent because the uniform velocity profile is the best approximation for the logarithmic velocity profile. Figure 5 shows the depth averaged hydraulic currents for the runs 5 and 6. No significant difference can be detected between the depth-averaged velocities in the two runs. Therefore, the parabolic velocity profile (Q3D model) seems to estimate the depth-averaged velocity quite well.

Figure 6 shows the difference between the two schemes used to approximate the value of the concentration at the face of the grid cell namely: 1st order upwinding scheme and QUICKEST scheme. After 1 hour of release of a 100ppm conservative pollutant at the inlet, the 1st order upwinding scheme exhibits higher numerical diffusion than the QUICKEST scheme.

Case Study: Lake Ontario

Lake Ontario is one of the Canadian Great Lakes and is used to demonstrate the applicability of the models. A uniform Cartesian horizontal grid of 4 Km spacing was constructed and the depth at the center of each grid element was obtained. The course grid enables choosing larger time step according to CFL criteria. The maximum depth of Lake Ontario for this domain is 227 meters, which makes the maximum possible time step to be 60 seconds in order to meet the stability requirement. Three discharge points on the grid are prescribed. The inflow of Niagara River 6880 $m^3 s^{-1}$ at grid point (14,3) and the outflows to the St. Lawrence river, 4118 $m^3 s^{-1}$ at grid point (75,23) and 2762 $m^3 s^{-1}$ at grid point (71,26).

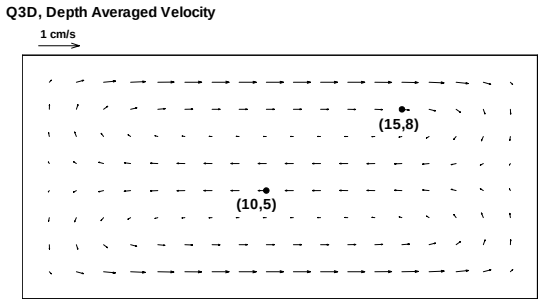

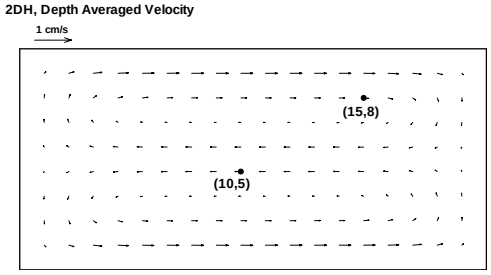

a) Circulation pattern after applying Q3D model *b) Circulation pattern after applying 2DH model*

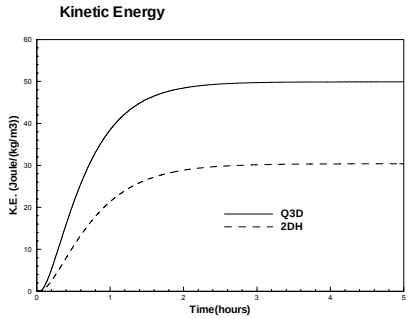

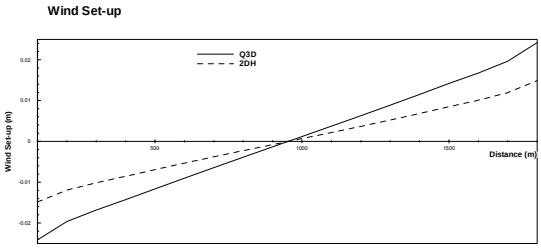

c) Total Kinetic Energy in both cases *d) Wind Set up in both cases*

Figure 2. Depth averaged wind induced current distribution and wind set-up in Basin-A for 5 m s^{-1} West Wind.

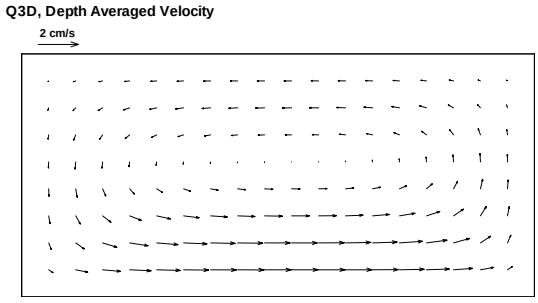

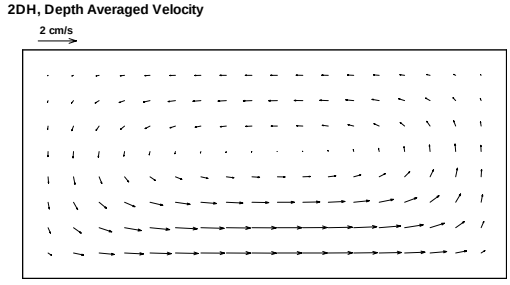

a) Circulation pattern after applying Q3D model *b) Circulation pattern after applying 2DH model*

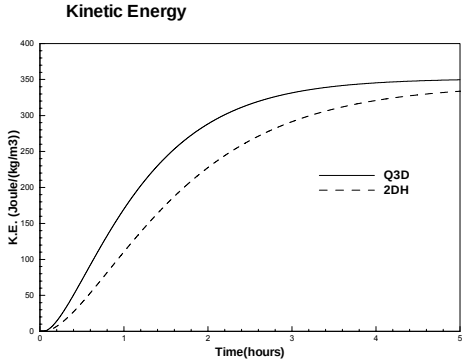

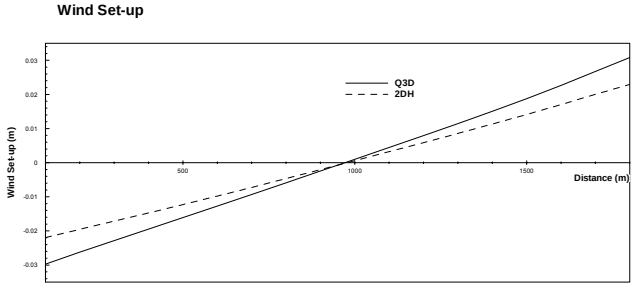

c) Total Kinetic Energy in both cases *d) Wind Set up in both cases*

Figure 3. Depth averaged wind induced current distribution and wind set-up in Basin-B for 5 m s^{-1} West Wind

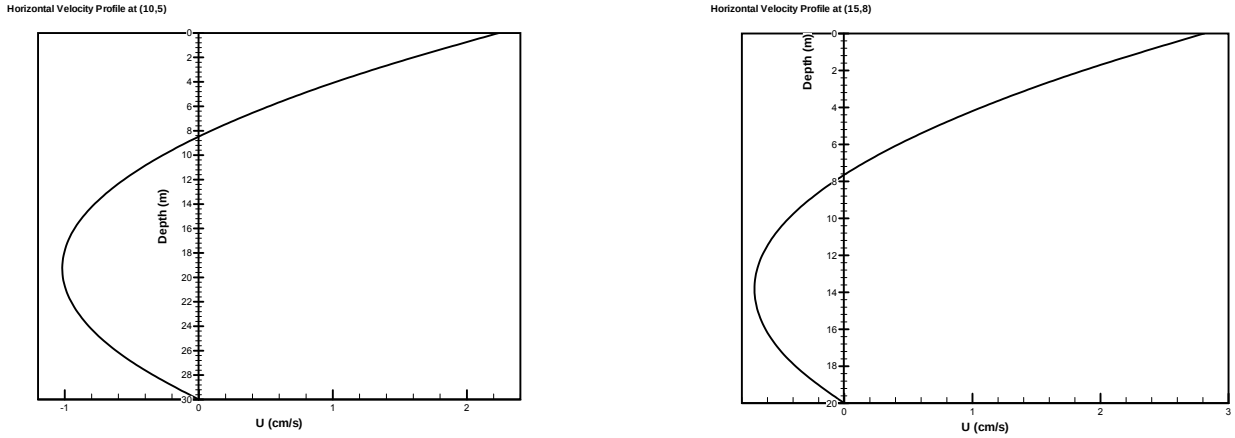

Figure 4. Vertical profile of the horizontal velocity in the direction of wind for Basin-A due to 5 m s^{-1} West Wind

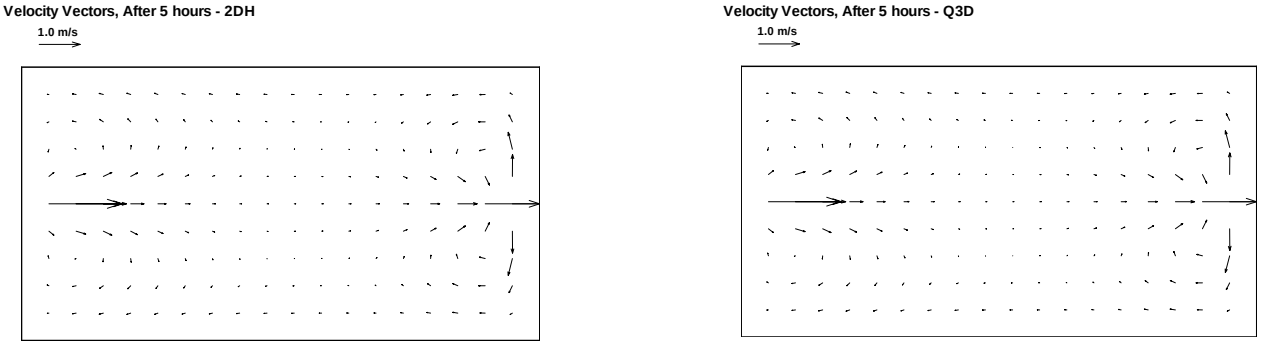

Figure 5. Depth averaged hydraulic current distribution for Basin-A under an inflow of 50 $m^3 s^{-1}$

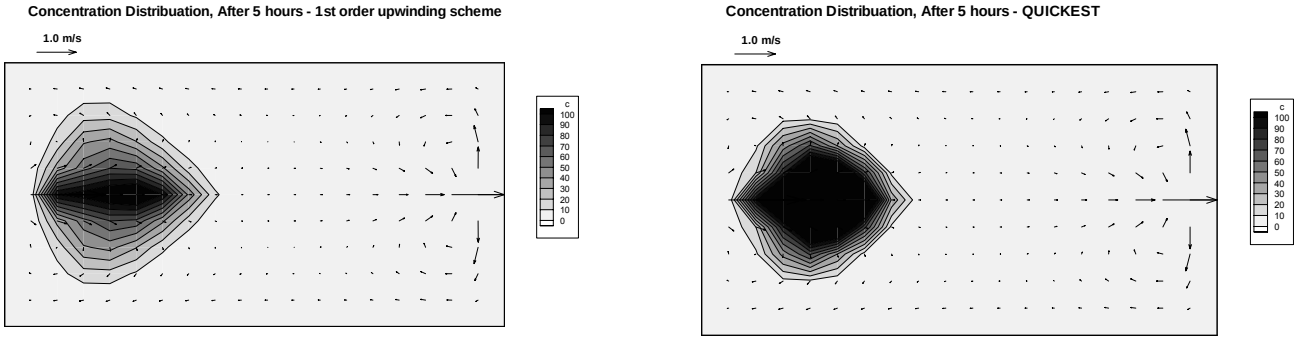

Figure 6. Equal concentration contours after 10 hours of the release of 100ppm conservative pollutant for 1-hour using 1st order upwinding scheme.

A numerical test for the hydrodynamic model of Lake Ontario found that the time step does not significantly affect neither the total kinetic energy of flow nor the time required to reach the steady state as long as the stability criteria is satisfied. To study the effect of the wind speed on the time to steady state, several runs were made to obtain the steady state time. All the runs were made using western winds. Table 3 shows the results of this study. It can be shown that it takes longer to reach steady state at lower wind speeds.

Table 3. The effect of wind speed on the time to steady state for Lake Ontario (Western Winds).

Wind Speed (m s^{-1})	Time to Steady State (hours)
40	38.10
30	58.4
20	94.0
10	130.0

Several runs were made for Lake Ontario in order to compare the results between the different models presented above. Table 4 summarizes these runs.

Table 4. Lake Ontario's runs.

Run #	Model Used		Time Step (s.)		Simulation (h.)		Release time (h.)	Force
	Hydr.	Poll.	Hydr.	Poll.	Hydr.	Poll.		
1	Q3D	---	30	---	200	---	---	5 m s^{-1} west wind
2	Q3D	---	30	---	200	---	---	10 m s^{-1} west wind
3	2DH	---	30	---	200	---	---	5 m s^{-1} west wind
4	Q3D	Up-wind	30	30	120	48	2 @ (18,18)	10 m s^{-1} west wind
5	Q3D	Up-wind	30	30	120	240	2 @ (18,18)	10 m s^{-1} west wind
6	Q3D	QUICKEST	30	30	120	48	2 @ (18,18)	10 m s^{-1} west wind
7	Q3D	QUICKEST	30	30	120	240	2 @ (18,18)	10 m s^{-1} west wind
8	Q3D	Up-wind	30	30	120	48	Cont. @ (18,18)	10 m s^{-1} west wind
9	Q3D	Up-wind	30	30	120	240	Cont. @ (18,18)	10 m s^{-1} west wind
10	Q3D	QUICKEST	30	30	120	48	Cont. @ (18,18)	10 m s^{-1} west wind
11	Q3D	QUICKEST	30	30	120	240	Cont. @ (18,18)	10 m s^{-1} west wind

Figure 7 shows the steady state circulation pattern in Lake Ontario due to 5m/s and 10m/s west wind respectively after applying the Q3D model. Four points have been selected to inspect the vertical velocity profile within the lake domain as shown in Figure 7. Figure 8, shows the vertical velocity profiles for the four selected points. It can be shown that strong return flows occurs at deep waters in the middle of the lake, while the shallow shores do not have return flows, which is consistent with the current structure identified by Simons (1973).
Figures 9 and 10 show the equal concentration contours after 2 and 10 days of the release of 100ppm of a conservative pollutant for 2 hours using the 1st order upwinding scheme and the QUICKEST scheme, respectively. The difference between the two schemes is clear after 10 days, where the numerical diffusion affects the former. In order to compare the performance of above schemes, the time-concentration curves at four points are shown in Figure 11. The difference between the two schemes is clear. The results of the two schemes for the case of instantaneous point source are given in Table 1. Generally, the spread and the time required for the pollutant to appear at the point T_i is less in the case of upwinding scheme.

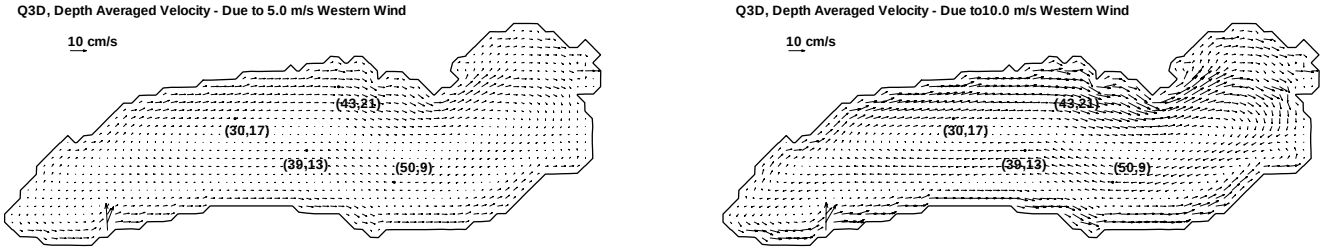

Figure 7. Steady State Circulation pattern in Lake Ontario due to 5 m s^{-1} and 10 m s^{-1} West Wind.

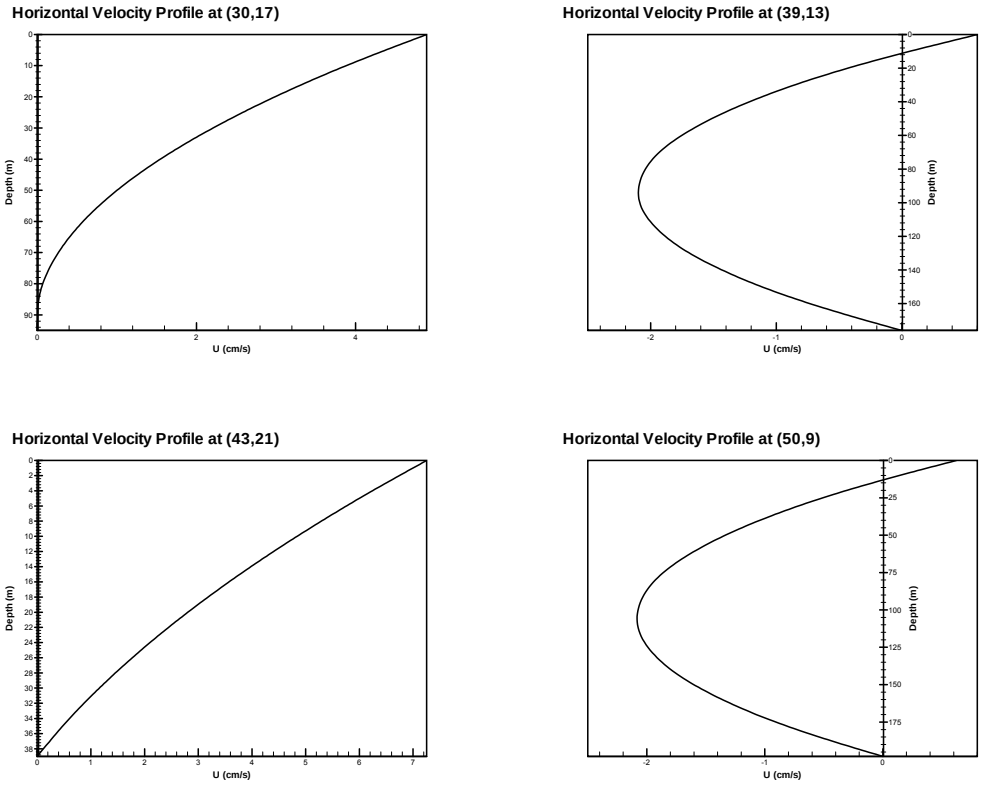

Figure 8. Vertical profile of the horizontal velocity in the direction of the wind, due to 5 m s^{-1} west wind (Run#1)

Figures 12 and 13 show the equal concentration contours after 2 and 10 days of the release of 100ppm of a conservative pollutant continuously using the 1st order upwinding scheme and the QUICKEST scheme, respectively. The difference between the two schemes is clear after 10 days since the pollutant reaches at a farther distance downstream for the case of the former scheme. Figure 14 shows the time concentration curves for the four points in the downstream path of the pollutant. The results of the two schemes for the case of continuous point source are shown in Table 6. The difference between the values of the final concentration (C_s) at a point C2 using both schemes are within 2.7%. The difference increases significantly further downstream for points C3, C4 and C5, where it reaches 220%. The 1st order upwinding overestimates the concentration for C3, C4 and C5 due to the numerical diffusion as the pollutant reaches the point much faster and accumulates earlier as shown in Figure 14.

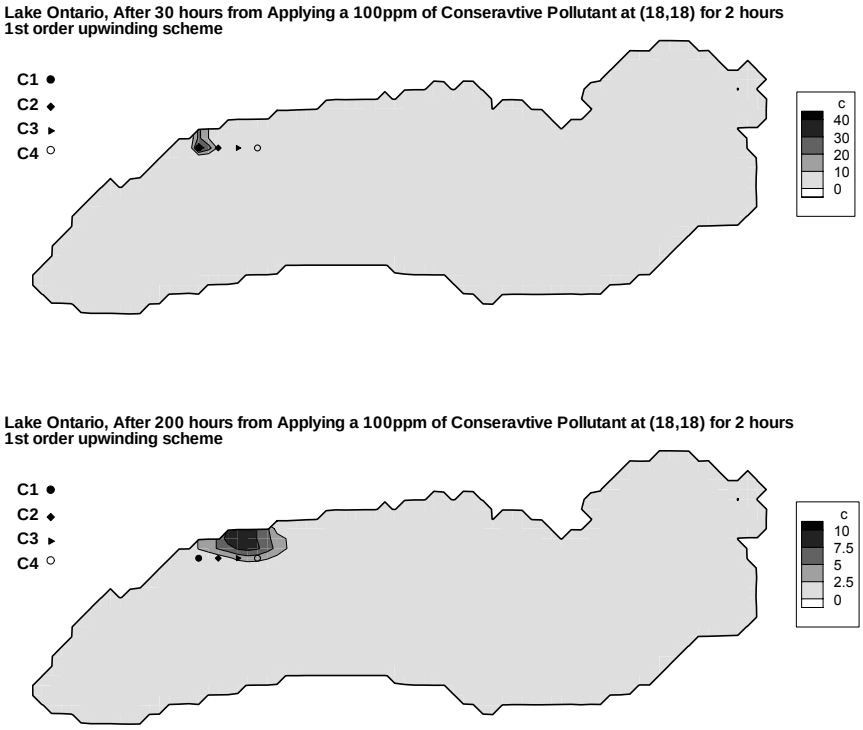

Figure 9. Equal concentration contours after 30 and 200 hours of the release of 100ppm conservative pollutant for 2-hours using 1st order upwinding scheme.

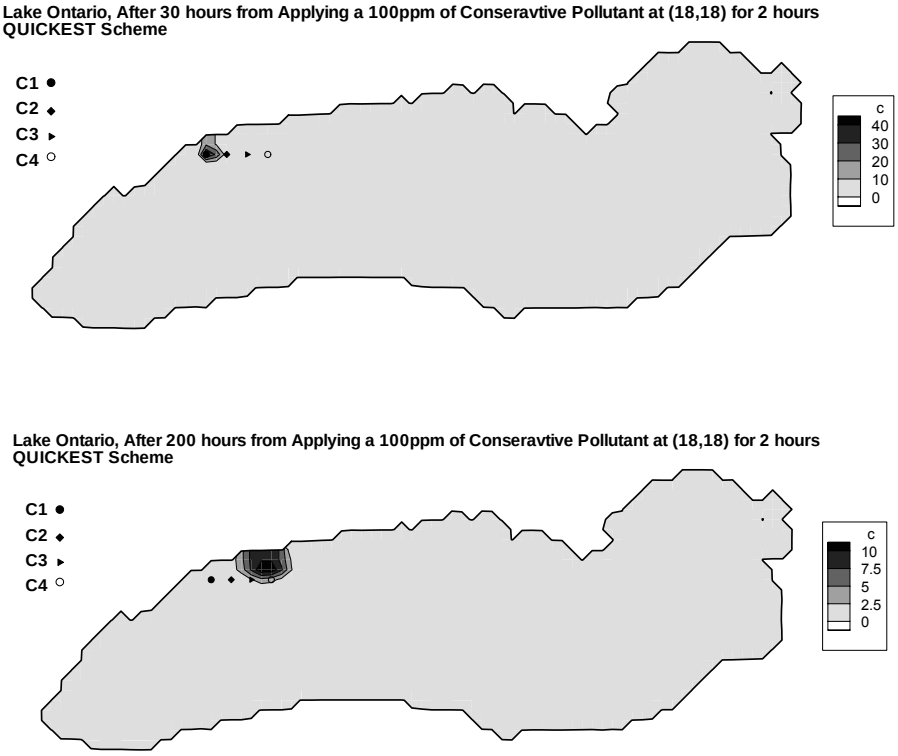

Figure 10. Equal concentration contours after 30 and 200 hours of the release of 100ppm conservative pollutant for 2-hours using QUICKEST scheme.

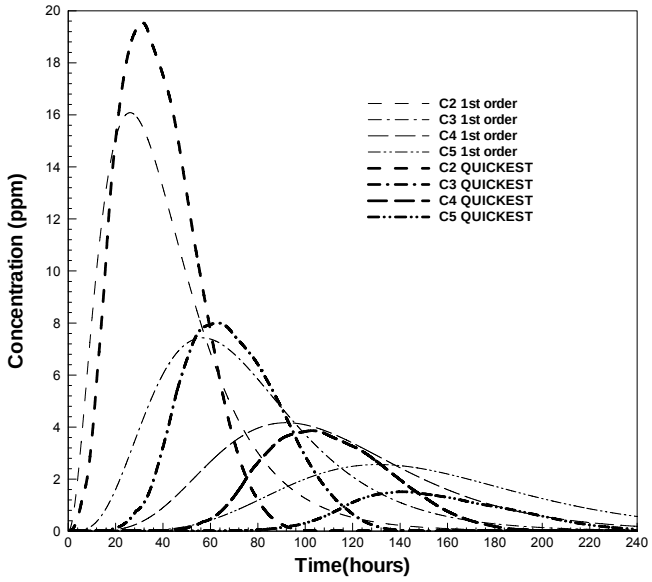

Figure 11. Time Concentration Curves for Points C2, C3, C4, and C5

Table 5. Comparison between 1st order upwinding scheme results and QUICKEST scheme results for the case of instantaneous point source.

Point	1st order Upwinding Scheme			QUICKEST Scheme		
	T_i (hours)	C_p (ppm)	T_p (hours)	T_i (hours)	C_p (ppm)	T_p (hours)
C2	0	16	25.3	0	19.6	30.5
C3	8.7	7.4	56.7	14.9	8.0	62.8
C4	20.6	4.16	89.4	40.5	3.85	101.8
C5	43.4	2.5	128	71.8	1.5	141

T_i: Time required for pollutant to appear at the point (hours).
T_p: Time at which the pollutant concentration reaches its maximum value (hours).
C_p: Peak concentration at the point (ppm).

Table 6. Comparison between 1st order upwinding scheme results and QUICKEST scheme results for the case of continuous point source.

Point	1st order Upwinding Scheme		QUICKEST Scheme	
	T_s (hours)	C_s (ppm)	T_s (hours)	C_s (ppm)
C2	107	62	85	63.7
C3	166	43.5	103	31.6
C4	240	32	146	17
C5	>240	23.1	194	7.2

T_s: Time required for the pollutant concentration to reach the steady state (hours).
C_s: Concentration of the pollutant at steady state (ppm).

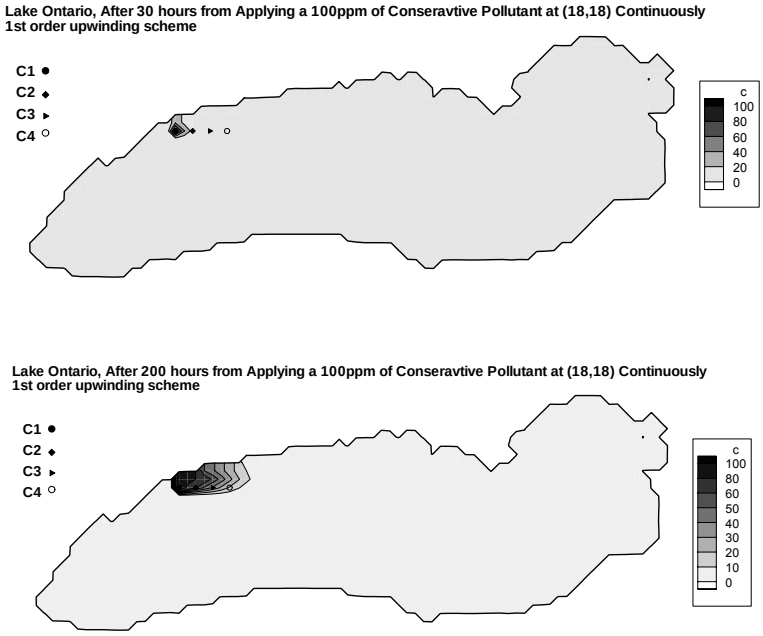

Figure 12. Equal concentration contours after 30 and 200 hours of the release of 100ppm conservative pollutant continuously using 1st order upwinding scheme.

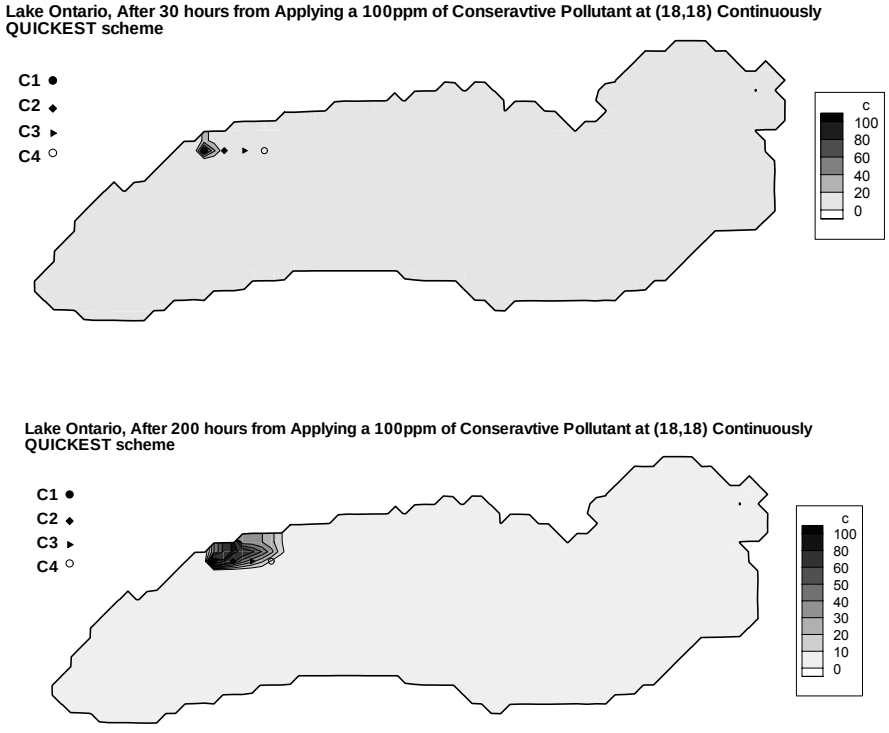

Figure 13. Equal concentration contours after 30 and 200 hours of the release of 100ppm conservative pollutant continuously using QUICKEST scheme.

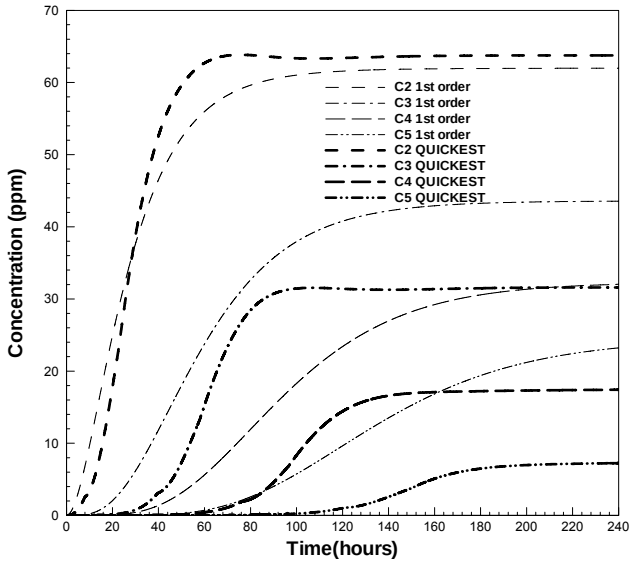

Figure 14. Time Concentration curves for points C2, C3, C4, and C5

CONCLUSIONS

Modeling the hydrodynamics and pollutant transport in lakes can be accomplished by using two-dimensional models that have the advantage of simplicity and reach good results in cases of hydraulically-induced circulation. Quasi-three-dimensional models can simulate both the hydraulically and wind-induced circulation by providing the depth-averaged circulation and the vertical current distribution. The 1st order upwinding scheme can be used for estimating pollutant concentrations near the pollutant source in the case of continuous point source. However, with increasing the transport time this scheme is greatly influenced by numerical diffusion resulting in inaccurate results. Higher order schemes such the QUICKEST scheme minimize the numerical diffusion and can estimate the pollutant concentration at these locations. The smoothing factor and the artificial horizontal eddy viscosity play important role in the hydrodynamics and have to be calibrated carefully for the grid size used in the simulation.

REFERENCES

Blaisdell, M.A., Tsanis, I.K., and Krestenitis, Y. (1991) Modeling the steady-state circulation in a distorted physical model of the Windermere Basin, Canadian Journal of Civil Engineering, Vol. 18- 5, 756-764.

Csanady, G.T. (1982) Circulation in the coastal ocean, D. Reidel Publishing Company, Dordrecht, Holland.

Ekman, V.W. (1905) On the influence of the earth's rotation on ocean currents, *Ark. Mat. Astro. Fys.*, **2**(11):1-53

Koutitas, C.G. (1988) Mathematical Models in Coastal Engineering, Pentech Press Limited, London.

Roache, P.J. (1972) Computational Fluid Dynamics, Hermosa Publishers, Albuquerque, NM.

Shen, H. and Tsanis, I.K. (1995) A three dimensional nested hydrodynamic/pollutant transport simulation model for the nearshore areas of Lake Ontario, *J. Great Lakes Res.,* **21**(2): 161-177

Simons, T.J., 1971, Development of numerical models of Lake Ontario, in *Proc. 14th Conf. Great Lakes Res.*, Internat. Assoc. Great Lakes Res, pp. 654-669.

Tsanis, I. K. and Wu, J. (1994) LMS – An Integrated Lake Modeling System, Environmental Software.

Tsanis, I.K. and Wu, J. (1991) Study of water currents in the Canadian Great Lakes, Atmospheric Service (AES) Report.

Wu, J. and Tsanis, I.K., (1991) *Quasi-three-dimensional modeling for Lake St. Clair,* 11th CSCE Annual Conference, May 29-31, Vancouver, B.C. pp. 26-35.

Wu J. (1993) An Integrated Hydrodynamic and Pollutant Transport Model for the Nearshore Areas of the Great Lakes and Their Tributaries, Ph.D. thesis, McMaster University, Department of Civil Engineering.